Recovery of quantum efficiency on Cs/O-activated GaN and GaAs photocathodes by thermal annealing in vacuum

Running title: Recovery of GaN and GaAs photocathodes by annealing

Running Authors: Daiki Sato et al.

Daiki Sato [1, 2, a)], Tomohiro Nishitani[2, 3], Yoshio Honda[3], and Hiroshi Amano[3]

[1]Nagoya University, Department of Electrical Engineering, Furo-cho, Chikusa-ku, Nagoya 464-8603, Japan

[2]Photo electron Soul Inc., Nagoya University Incubation Facility, Furo-cho, Chikusa-ku, Nagoya 464-0814, Japan

[3]Nagoya University, Center for Integrated Research of Future Electronics, Institute of Materials and Systems for Sustainability, Furo-cho, Chikusa-ku, Nagoya 464-8601, Japan

[a)] Electronic mail: satou.daiki@d.mbox.nagoya-u.ac.jp

In this paper, we describe the effectiveness of thermal annealing in vacuum for quantum efficiency (QE) recovery from Cs/O-activated GaN and GaAs photocathodes. The QE of Cs/O-activated GaN photocathode at 3.4 eV dropped from 1.0% to < 0.001% upon exposure to nitrogen, and then increased to 0.6% upon annealing. On the other hand, the QE of Cs/O-activated GaAs at 1.42 eV did not increase after the annealing. In addition, after Cs/O activation, the sample was exposed to normal laboratory-air and installed in an X-ray photoemission spectroscopy system. Upon annealing at 330°C, three key results were confirmed as follows: (1) the work function decreased by 0.32 eV, (2) the chemical states of Cs 4*d* and Ga 3*d* were unchanged, and (3) the intensities of O 1*s* and C 1*s* on the high-binding-energy side decreased. In conclusion, the experimental results indicate that the annealing recovers the QE of Cs/O-activated GaN photocathode.

I. INTRODUCTION

Semiconductor photocathodes having a negative electron affinity (NEA) state have the advantage of a large current with low emittance and a multielectron beam. The mechanism of photoemission from an NEA photocathode involves three steps: 1) photoexcitation of electrons from the valence band to the conduction band, 2) diffusion of electrons to the surface, and 3) escape of electrons.[1,2] The electron sources used in industrial applications are mainly thermal and field emitters. The energy distribution and emittance of photocathodes are less than 0.3 eV[3] and 0.1 μm rad,[4] respectively, which are lower than those of thermal and field emitters. In addition, a photocathode can create a high current of larger than 1 mA.[5] From these features, the brightness of a photocathode can reach 10^8 $Acm^{-2}sr^{-1}$ at an acceleration voltage of 3 kV.[6] These advantages of photocathodes can improve the throughputs of semiconductor manufacturing processes such as defect inspection and electron beam lithography.

GaN-based photocathodes are suitable for industrial applications. NEA semiconductor photocathodes fabricated using GaAs are used as electron sources in high-energy research.[7] However, since the NEA surface of a GaAs photocathode is sensitive to gas adsorption,[8] the surrounding area should be kept in a vacuum where the pressure is lower than 10^{-9} Pa. Therefore, it is difficult to use such a photocathode in industrial equipment with a vacuum pressure of higher than 10^{-6} Pa. On the other hand, wide-gap semiconductors such as GaN and InGaN are attractive candidates because they have longer lifetimes (more than 10 times longer).[9,10]

The electron source desired for industrial equipment can be used in an environment with a vacuum pressure of 10^{-6} Pa or higher. Ultimately, an electron source that can withstand atmospheric exposure is ideal. However, there have been no studies on the effects of atmospheric exposure on GaN and GaAs photocathodes. The purpose of this study was to investigate the effects of atmospheric pressure gas and annealing on Cs/O-activated GaN and GaAs photocathodes (hereafter, Cs/O GaN and Cs/O GaAs, respectively). Changes in the quantum efficiency (QE) of Cs/O GaN and Cs/O GaAs owing to atmospheric-pressure nitrogen exposure, followed by annealing in vacuum were measured. In addition, changes in the work function and the core levels (Ga 3*d*, Cs 4*d*, O 1*s*, C 1*s*) of the laboratory-air-exposed Cs/O GaN were investigated by X-ray photoemission spectroscopy (XPS).

II. EXPERIMENTAL

A. Sample preparation

Figure 1 shows the structure of the GaN photocathode. p-Type Mg-doped GaN was grown by metal-organic chemical vapor deposition. The p-type layer was grown on a sapphire substrate with undoped GaN as the buffer layer. The thickness of the p-type layer, which was calculated from the growth rate, was 200 nm. The sample was annealed at 700°C in atmosphere for p-type activation. After activation, a hole concentration of 2.0×10^{18} cm^{-3} was measured on the basis of the Hall effect. Then, the sample was rinsed with acetone and methanol.

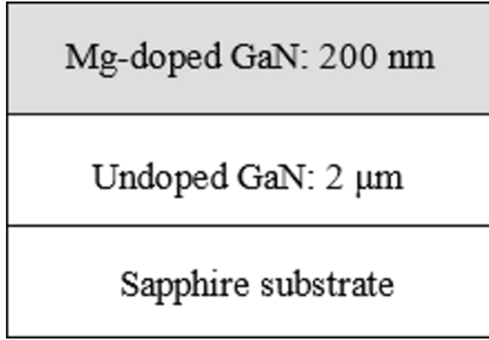

FIG. 1. Structure of GaN photocathode.

The GaAs was manufactured by Hitachi Cable, Ltd., and the doping concentration of Zn and the film thickness were 1 to 3×10^{19} cm^{-3} and 300 μm, respectively. The sample was rinsed with acetone and methanol.

B. *Surface activation by cesium and oxygen deposition*

The surface of GaN was activated by alternate Cs and O_2 deposition in an ultrahigh-vacuum chamber. The photocathode test system at Nagoya University was used for the experiment and is schematically shown in Fig. 2. The details of the system were reported elsewhere.[11,12] In brief, the system consists of two parts: a Cs deposition chamber for activation and a load lock chamber for sample installation. The base pressures of the Cs deposition chamber and load lock chamber were 5×10^{-9} Pa and 1×10^{-6} Pa, respectively. The samples were cleaned prior to Cs deposition by heating for 1 h in the Cs deposition chamber to remove water and oxide impurities on the sample. The cleaning temperatures of GaN and GaAs were 600°C and 500°C, respectively. The temperature of the sample surface was monitored using an uncorrected optical pyrometer as viewed though a view port. The minimum detection limit of the pyrometer was 200°C. After the cleaning, the surface was activated at room temperature by the "yo-yo" method,

where Cs and O_2 were alternately deposited three times.[13] To monitor the photocurrent during the activation, an acceleration voltage of -100 V was applied to the sample. QE was calculated using Eq. (1),

$$QE = 1240 \times \frac{I}{P\lambda}, \quad (1)$$

where I is the emission current, P is the power of incident light, and λ is the wavelength of incident light. Cs and O_2 were deposited at room temperature.

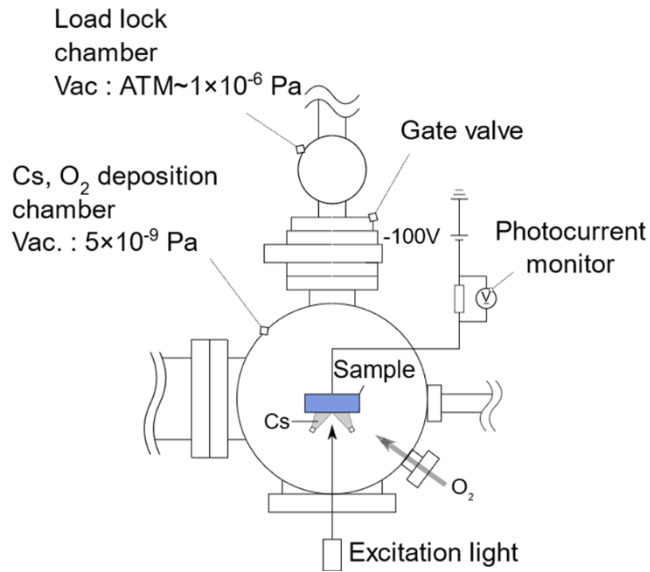

FIG. 2. Schematic illustration of photocathode test system.

C. Nitrogen exposure and anneal treatment in vacuum

Figure 3 shows the basic flow of the experiment. Cs/O GaN and Cs/O GaAs were used for the experiment.

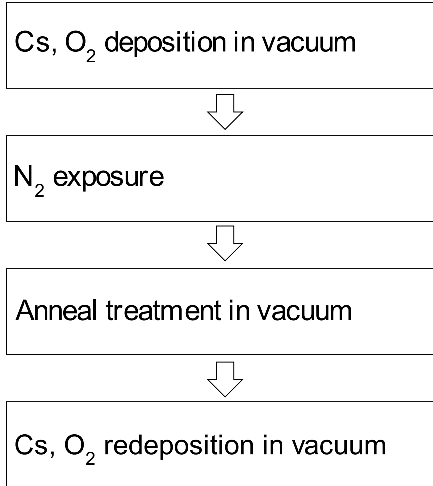

FIG. 3. Flow of the experiment. The excitation energy dependence of QE was measured at each stage.

After the activation, the samples were transferred to a load lock chamber and exposed to pure N_2 (>99.99995%) at a pressure of 0.3 MPa for 1 min. After the exposure, the sample was transferred to the Cs deposition chamber and annealed at a base pressure of 5×10^{-9} Pa. The heater power was increased while measuring the QE. Figure 4 shows the changes in heater power with time for Cs/O GaN and Cs/O GaAs. The heater power was increased while monitoring the increase in QE with the sample temperature, and the heater power was turned off when the increase in QE saturated. After annealing, Cs and O_2 were redeposited on the semiconductor surface, and QE was evaluated to confirm the damage to the surface caused by the annealing. The excitation energy dependences of QE were measured before nitrogen exposure, after annealing, and after the redeposition of Cs and O_2.

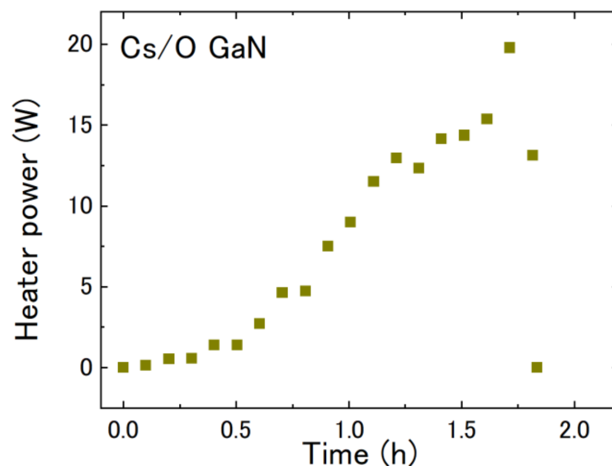

(a)

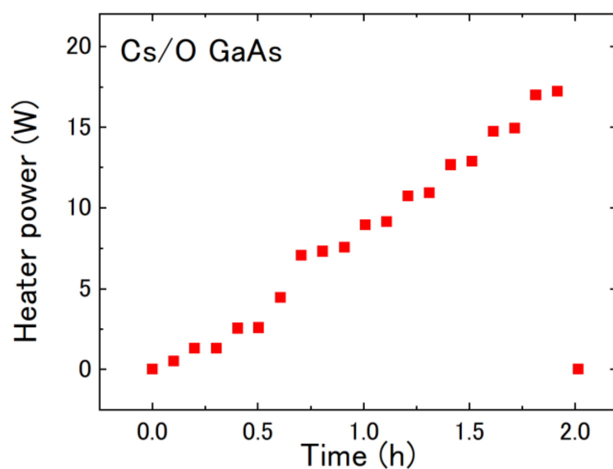

(b)

FIG. 4. Time variation of heater power for vacuum annealing. (a) shows changes for Cs/O GaN, and (b) shows changes for Cs/O GaAs.

D. Measurement of work function and chemical shift by XPS

Figure 5 shows a basic flow of the measurement of work functions and core levels. Cs/O GaN was used for the investigation.

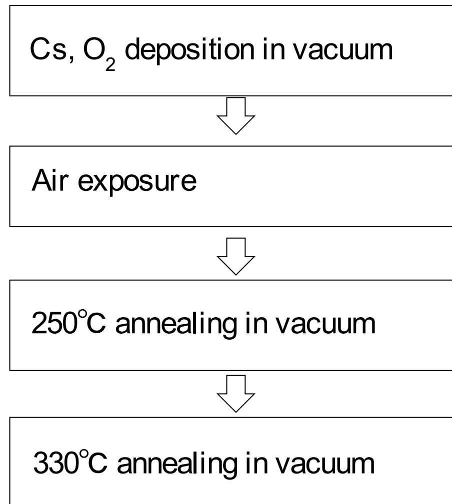

FIG. 5. Flow of the experiment. The work function and energy core levels were measured before and after the annealing.

After the Cs deposition, the sample was exposed to laboratory-air for 1 h prior to storage in a vacuum desiccator, transported to Aichi Synchrotron Center BL7U, exposed to laboratory-air again for 1 h, then installed in an XPS system.[14] The XPS system consisted of three vacuum chambers: (1) a load lock chamber, (2) an annealing chamber, and (3) an analysis chamber for XPS. Figure 6 shows a schematic of the XPS system. An MBS A-1 hemispherical energy analyzer manufactured by MB SCIENTIFIC AB with a 200 mm mean radius was used. The beam size at the sample position was 0.1 mm × 0.4 mm. The base pressures in the main chamber and annealing chambers were both 5×10^{-8} Pa. The resolution of the analyzer was 40 meV at an electron energy of 200 eV. The work function of the analyzer was predetermined to be 4.35 eV by Au Fermi level measurement.

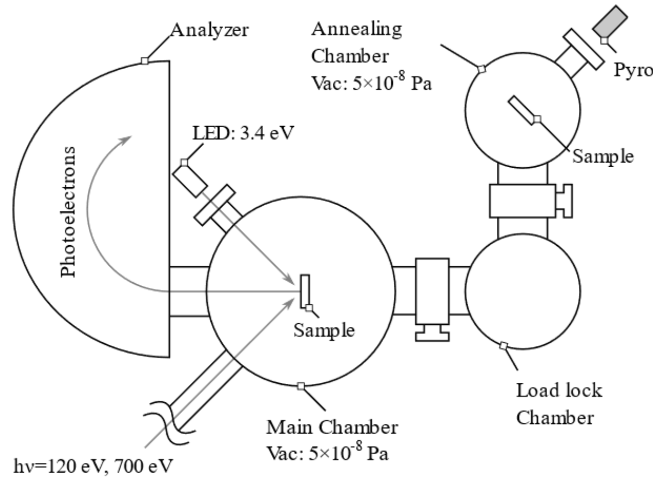

FIG. 6. Schematic of XPS system at Aichi SR BL7U.

The work function energy distribution curves (WDC) and energy core levels of Cs 4*d*, Ga 3*d*, O 1*s*, and C 1*s* were obtained before and after the annealing. Firstly, an ultraviolet light-emitting diode with hν = 3.40 ±0.05 eV was used for the WDC measurement. To reduce the influence of the surface photovoltage effect (SPV) on the WDC measurement, the power density of the excitation light was set to $2.2 \pm 0.4 \times 10^{-3}$ W/cm^2 (70 ±10 μW in a 2-mm-diameter spot). G. A. Mulhollan *et al.*, have shown that the power density which induced the SPV was in the range of 1–150 W/cm^2 for GaAs photocathode[15], so the SPV effect can be ignored in our experiment. A bias voltage of -20 V was applied to the sample holder to detect photoelectrons having kinetic energies below the work function of the analyzer. Figure 7 shows the potential diagram between GaN and the energy analyzer for the WDC measurement under the applied bias. E_{CBM}, E_{CBM}, and E_F are the conduction band minimum, valence band maximum, and Fermi level, respectively. VL is the vacuum level of the surface. The work function (Φ) of the surface was determined as the energy from E_F to the threshold of the WDC, where the threshold was determined as the lower energy at 10% of the peak value. Secondly, the

sample was irradiated with X-rays having energies of 120 eV and 700 eV. To obtain information on the Cs 4*d* and Ga 3*d* core-level shifts slightly below the surface, hν = 120 eV was chosen. On the other hand, hν = 700 eV was chosen to obtain information on the O 1*s* and C 1*s* core-level shifts. These experiments were conducted at room temperature before and after annealing at 250°C and 330°C for 30 minutes. Table I gives the reference binding energies of the core levels.[16-18]

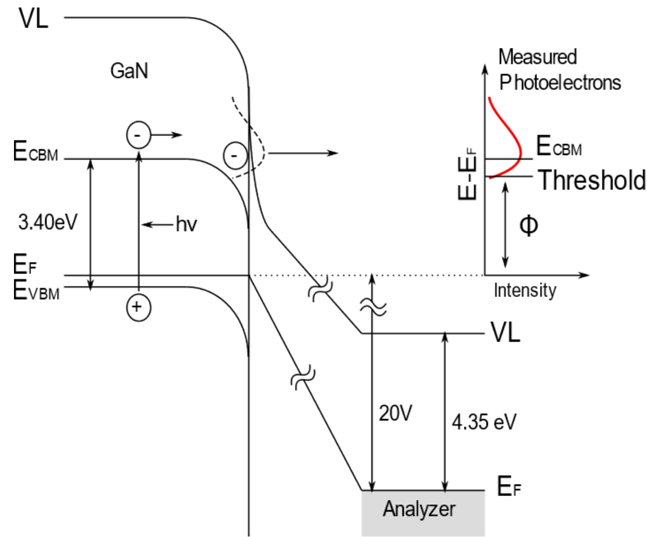

FIG. 7. Potential diagram for the entire structure under the applied bias: E_{CBM}, E_{VBM}, E_F, and Φ are the conduction band minimum, valence band maximum, Fermi level of the semiconductor, and the work function of Cs/O GaN, respectively. VL is the vacuum level of the surface.

TABLE I. Reference binding energies for core levels

Ga	Cs	C 1*s*[17]		O 1*s*	
$3d_{5/2}$[16]	$4d_{5/2}$[16]	C-C	C-O	Cs_2O_2[18]	C=O[17]
20.0 eV	79.0 eV	284.8 eV	286.3 eV	530.3 eV	531.0eV

III. RESULTS AND DISCUSSION

A. Effect of nitrogen exposure and anneal treatment on Cs/O-activated photocathode

The changes in QE of Cs/O GaN are shown in Fig. 8 (a) as a function of time and applied annealing temperature at an excitation of 3.4 eV. The initial QE was 1.0%; this value decreased to below the measurement limit immediately upon exposure to N_2 at 0.2 MPa. QE recovered with the application of a 200℃ annealing. Continued heating to 330℃ further increased QE to a maximum of 0.6%, where it remained stable after heating.

The change in QE of Cs/O GaAs with annealing time is shown in Fig. 8 (b). QE at the excitation energy of 3.4 eV was 5.0% immediately after the surface activation and decreased to 4.3×10^{-3}% by nitrogen exposure. Thereafter, the surface temperature and QE increased with the increase in heater power, as shown in Fig. 4 (b). Two hours after annealing, when the temperature reached 450°C, QE recovered to 3.8% and then saturated.

The change in QE as a function of excitation energy is also shown in Fig. 8 (a) for Cs/O GaN. The maximum change in QE was calculated from the differential value, which was determined as the threshold. QE for Cs/O GaN reached a maximum of 2.1% at an excitation energy of 3.5 eV. The threshold was 3.39 eV, at which QE was 1.0%. Upon exposure to nitrogen, QE dropped below the detection limit. After annealing to 330℃, QE remained low below an excitation energy of 3.0 eV. Additional deposition of cesium and oxygen led to the full recover of the QE response curve.

Figure. 9 (a) shows the excitation energy dependence of the QE of Cs/O GaAs. The threshold was 1.41 eV immediately after the activation, and QE was 0.17% at the threshold. QE increased rapidly until the excitation energy reached the threshold, and then slowly increased. QE reached a maximum of 4.7% at an excitation energy of 3.3 eV. After nitrogen exposure, QE dropped below the measurement limit. After annealing at 450°C in vacuum, QE recovered, and the threshold shifted to 3.35 eV. QE increased gradually with increasing energy and showed a maximum value of 0.29%. Recovery of QE was not observed at 1.42 eV, which is the band gap of GaAs. After that, Cs and O were deposited again, and QE was completely recovered. The changes in QE for the two photocathodes are summarized in Table II.

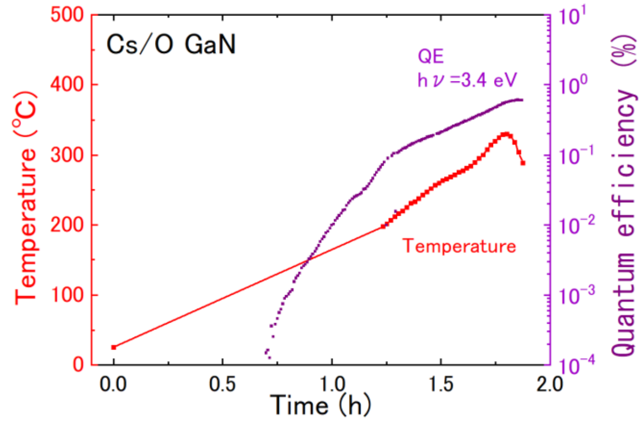

(a)

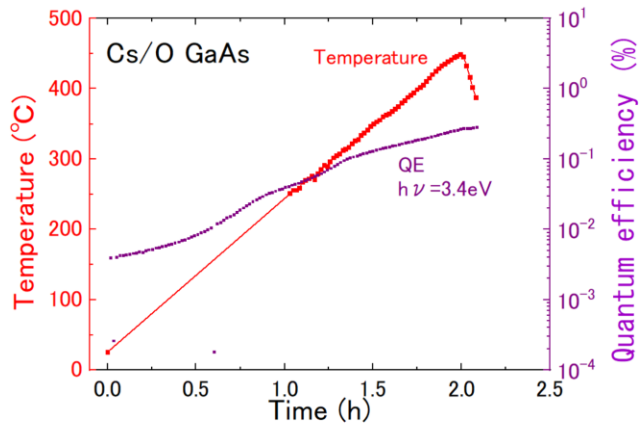

(b)

FIG. 8. QE and applied annealing temperature as functions of time. (a) shows changes for Cs/O GaN and (b) shows changes for Cs/O GaAs. The temperature was measured using a pyrometer with a minimum detection limit of 200°C. The changes in heater power are shown in Fig. 4.

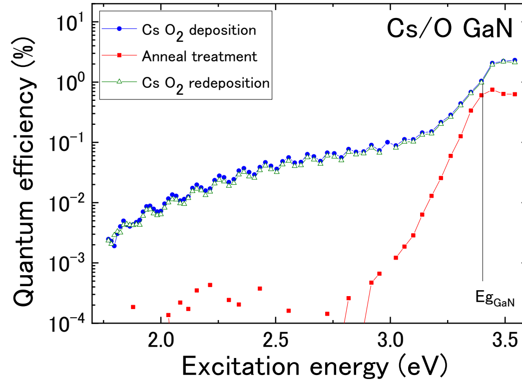

(a)

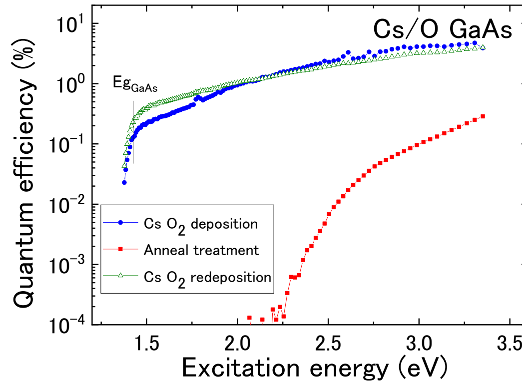

(b)

FIG. 9. Changes in QE spectrum after Cs and O_2 deposition, annealing, and Cs and O_2 redeposition. (a) shows spectra for Cs/O GaN and (b) shows spectra for Cs/O GaAs. Eg_{GaN} and Eg_{GaAs} indicate the band gap of GaN and GaAs, respectively.

TABLE II. Changes in QE of GaN and GaAs after anneal treatment

		Quantum efficiency [%]			
Semiconductor	Excitation energy [eV]	After Cs, O_2 deposition	After N_2 exposure	After annealing	After Cs, O_2 redeposition
GaN	3.40	1.0	<0.001	0.6	1.0

GaAs	1.42	0.1	<0.001	<0.001	0.23
	3.40	5.0	0.0043	0.28	3.8

B. Measurement of work function and chemical shift by XPS

Figure 10 shows the WDC obtained from Cs/O GaN before and after annealing at 250°C and 330°C. The horizontal axis shows the electron energy above the Fermi level of the sample. The position of the p-GaN bulk conduction band maximum (E_{CBM}) was estimated from the carrier density calculated from the results of Hall measurement. The calculated E_{CBM} at 3.3 eV is shown in Fig. 10. First, the integrated intensity of the WDC more than doubled after annealing at 250°C and increased more than 12-fold after annealing at 330°C. Second, the work function decreased by 0.17 eV after annealing at 250°C and by 0.32 eV after annealing at 330°C. Table III shows the work function and the integrated intensity of the WDC.

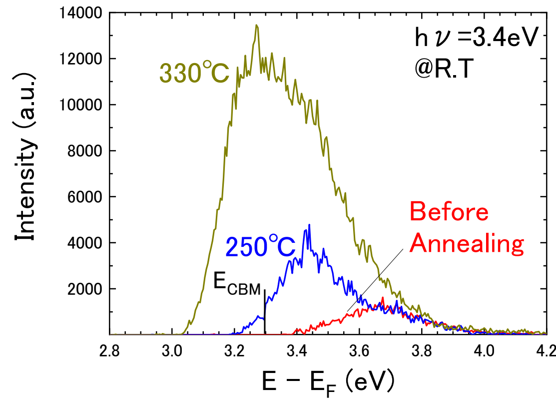

FIG. 10. Work function energy distribution curves obtained from GaN before and after annealing. The excitation energy was 3.40 eV and the applied voltage was -20 V. The conduction band maximum of the sample is labeled as E_{CBM}, which was estimated from the carrier density of the sample.

Figure 11 shows the core-level spectra for (a) Ga 3*d*, (b) Cs 4*d*, (c) O 1*s*, and (d) C 1*s*. The intensities of photoelectrons were normalized by the peak intensity of Ga 3*d*. Ga 3*d* and Cs 4*d* were measured with a photon energy of 120 eV. The chemical shifts of Ga 3*d* and Cs 4*d* were less than 60 meV upon the anneal treatment. Annealing at 250°C and 330°C decreased the peak intensities of Cs 4*d* to 94% and 75%, respectively. For O 1*s* and C 1*s*, the experimental results were evaluated referring to the binding energies of C-C, C-O, Cs_2O_2, and C=O.[17,18] The peak intensity of Cs_2O_2 (O 1*s*), decreased to 99% and 97% and that of intensity of C=O (O 1*s*) decreased to 44% and 37% after annealing at 250°C and 330°C, respectively. The peak intensity of C-C (C 1*s*) did not decrease after 250°C annealing but decreased to 55% after 330°C annealing. The peak intensity of C-O (C 1*s*) decreased to 76% and 0% after annealing at 250°C and 330°C, respectively. Table III also shows the XPS intensities for Cs 4*d*, C 1*s*, and O 1*s*.

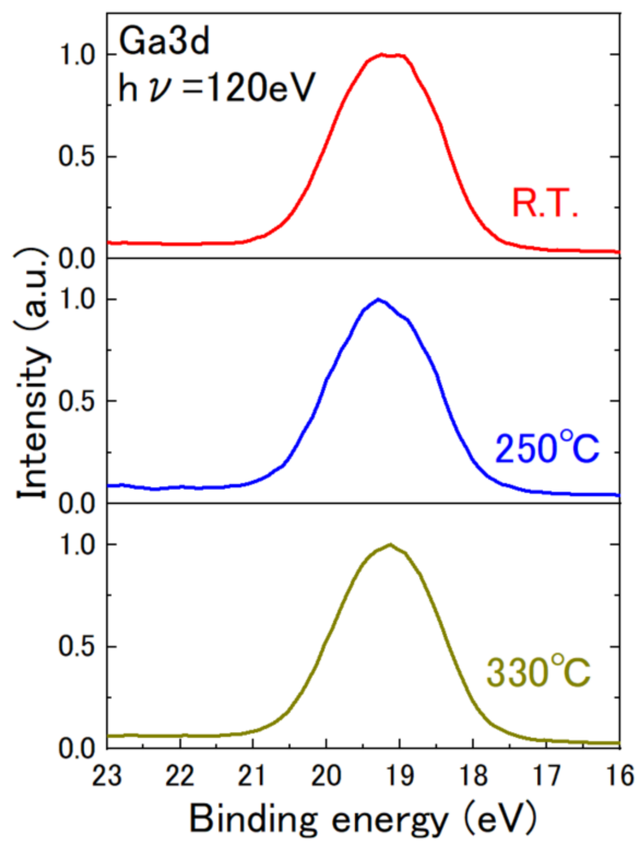

(a)

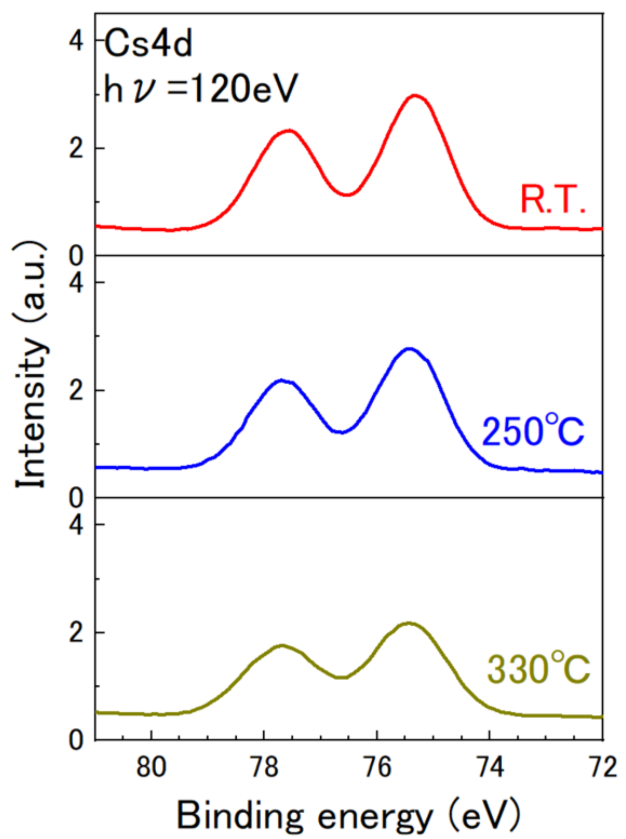

(b)

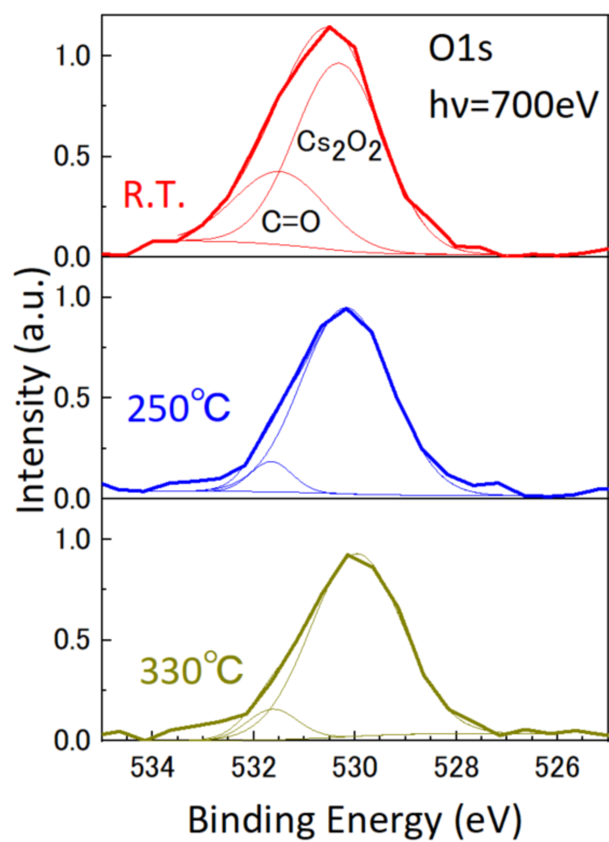

(c)

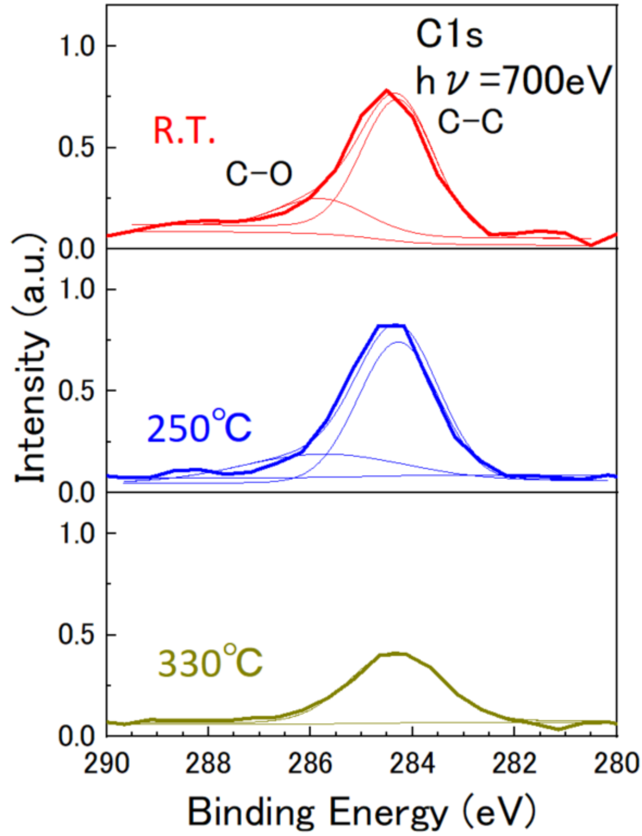

(d)

FIG. 11. (a) Ga 3*d*, (b) Cs 4*d*, (c) O 1*s*, and (d) C 1*s* spectra before annealing and after annealing at 250°C and 330°C. Intensities are normalized by the peak value of Ga 3*d*.

TABLE III. Summary of WDC and XPS results before and after annealing

	WDC		XPS peak intensity (normalized by the peak value of Ga 3*d*)				
				O 1*s*		C 1*s*	
	Work function (shift)[eV]	Integrated intensity	Cs $4d_{5/2}$	Cs_2O_2	C=O	C-C	C-O
Room temperature	3.44 (±0)	390	2.32	0.96	0.43	0.74	0.25
250°C	3.26 (−0.18)	1130	2.18	0.95	0.19	0.74	0.19
330°C	3.09 (−0.35)	4990	1.74	0.93	0.16	0.41	0

C. Discussion

From the experimental results shown above, we concluded that the annealing causes CO and CO_2 to desorb from the surface of the degraded GaN photocathode, then QE was recovered by the lowering of the work function, where the electron affinity became negative. Chanlek *et al*. have shown that the absorption of O_2, CO, and CO_2 degrades NEA surfaces.[8] Since the atmosphere contains these gas species, the surface degradation observed in this study should be caused by their adsorption. Also, during N_2 exposure, impurities on the inner wall of the chamber, which is the nitrogen filling path, adsorb on the GaN surface. According to a report by Iijima *et al.*, the desorption temperature of CO and CO_2 chemisorbed on the surface of a GaAs photocathode is between 150°C and 300°C.[19] This temperature range is in good agreement with the temperature for QE recovery from our results. No chemical shifts of Ga 3*d* and Cs 4*d* were found in the recovery of QE. This may be because the influences of CO and CO_2 are below the XPS measurement resolution.

Unlike in Cs/O GaN, the reason why the QE of Cs/O GaAs at the band edge was not recovered by annealing may be that the electron affinity did not become negative even with anneal treatment. Since the electron affinity of p-GaAs (= 3.4 eV) is about 1.3 eV larger than that (= 2.1 eV) of p-GaN, the electron affinity may not be negative only upon the reduction in the work function with the desorption of CO and CO_2. In addition, in Cs/O GaN and Cs/O GaAs, the excitation energy dependence of QE became similar to that before nitrogen exposure upon the redeposition of Cs and O_2 after annealing. From these results, the exposure and annealing did not damage the semiconductor surface of

both samples. On the basis of the above, the Cs/O GaN photocathode was found to be superior to the Cs/O GaAs photocathode not only in terms of its long lifetime but also in the recovery rate upon the anneal treatment.

The XPS results show that the intensity of Cs decreased upon annealing. The reason why QE did not recover to 100% after annealing, as shown in Fig. 9 (a), can be described by the finding that part of the Cs also desorbed during the annealing. Moreover, as shown in Fig. 9 (a), there was no recovery of QE on the low-energy side after annealing. The work function of Cs oxide including Cs was reported to be 1.3 – 2.0 eV.[20] From these findings, the low-energy photoelectrons in Fig. 9 (a) may be generated from Cs and Cs oxide. The reason why the QE from the lower-energy side was not recovered by nitrogen exposure and annealing may be that Cs and Cs oxide, which contribute to the generation of low-energy photoelectrons, were desorbed from the surface during the annealing. Even in the absence of such species of Cs and Cs oxide, the surface after annealing exhibits 60% of the original QE. Therefore, the Cs desorbed during the annealing may be from the outermost surface, which has a weak interaction with Ga.

IV. SUMMARY AND CONCLUSIONS

It was clarified that the exposure of Cs/O GaN to nitrogen decreased its QE by more than three orders of magnitude. It was also confirmed that the QE of degraded Cs/O GaN was recovered by annealing in vacuum. The QE of Cs/O GaN at 3.40 eV changed from 1.0% before N_2 exposure to <0.001% after N_2 exposure and 0.6% after the anneal treatment. The QE of GaAs at the band edge was not recovered by the anneal treatment. The changes in the work function and the energy core levels of the Cs/O GaN surface

were investigated using XPS. Regarding the annealing at 330°C, the following three key results were obtained: (1) the work function decreased by 0.32 eV, (2) the chemical states of Cs 4*d* and Ga 3*d* were unchanged, and (3) the intensities of O 1*s* and C 1*s* on the high-binding-energy side decreased. These experimental results suggest that upon annealing a degraded GaN photocathode, CO and CO_2 desorb from the surface, then the functional surface is recovered by the reduction in the work function.

ACKNOWLEDGMENTS

The authors thank the staff of the Aichi Synchrotron Center, especially Dr. M. Nakatake, for the operation of the XPS system and the helpful advice. This work was supported by SENTAN, JST.

[1]W. E. Spicer, Phys. Rev. **112**, 114 (1958).

[2]W. E. Spicer, Appl. Phys. **12**, 115 (1957).

[3]D. A. Orlov, U. Weigel, D. Schwalm, A. S. Terekhov, and A. Wolf, Nucl. Instrum. Methods Phys. Res., Sect. A **532**, 418 (2004).

[4]A. W. Baum, W. E. Spicer, R. F. W. Pease, K. A. Costello, and V. W. Aebi, Proc. SPIE **2550**, 189 (1995).

[5]J. Grames, P. Adderley, L. Brittian, D. Charles, J. Clark, J. Hansknecht, M. Poelker, M. Stutzman, and K. Surles-Law, in Proceedings of 2005 Particle Accelerator Conference, May 16-20, Knoxville (IEEE, Piscataway, 2005), p. 2875.

[6]A. W. Baum, W. E. Spicer, R. F. W. Pease, K. A. Costello, and V. W. Aebi, Proc. SPIE **2522**, 208 (1995).

[7]SLD Collaboration, Phys. Rev. Lett. **70**, 2515 (1993).

[8]N. Chanlek, J. D. Herbert, R. M. Jones, L. B. Jones, K. J. Middleman, and B. L. Militsyn, J. Phys. D: Appl. Phys. **47**, 055110 (2014).

[9]T. Nishitani, M. Tabuchi, H. Amano, T. Maekawa, M. Kuwahara, and T. Meguro, J. Vac. Sci. B **32**, 06F901 (2014).

[10]F. Machuca, Z. Liu, J. R. Maldonado, S. T. Coyle, P. Pianetta, and R. F. W. Pease, J. Vac. Sci. B **22**, 3565 (2004).

[11]T. Nishitani, M. Tabuchi, K. Motoki, T. Takashima, A. Era, and Y. Takeda, J. Phys.: Conf. Ser. **298**, 012010 (2011).

[12]D. Sato, T. Nishitani, Y. Honda, and H. Amano, Jpn. J. Appl. Phys. **55**, 05FH05 (2016).

[13]M. Kuriki, C. Shonaka, H. Iijima, D. Kubo, H. Okamoto, H. Higaki, K. Ito, M. Yamamoto, T. Konomi, S. Okumi, M. Kuwahara, and T. Nakanishi, Nucl. Instrum. Methods Phys. Res., Sect. A **637**, S87-S90 (2011).

[14]N. Isomura, M. Kamada, T. Nonaka, E. Nakamura, T. Takano, H. Sugiyama, and Y. Kimoto, J. Synchrotron Radiat. **23**, 281 (2016).

[15]G. A. Mulhollan, A. V. Subashiev, J. E. Clendenin, E. L. Garwin, R. E. Kirby, T. Maruyama, and R. Prepost, Phys. Lett. A **282**, 309 (2001).

[16]D. Briggs, *Handbook of X-ray and ultraviolet photoelectron spectroscopy* (Heyden, London, 1977).

[17]J. Landoulsi, M. J. Genet, S. Fleith, Y. Touré, I. Liascukiene, C. Méthivier, and P. G. Rouxhet, Appl. Surf. Sci., **383**, 7183 (2016).

[18]J. Hrbek, Y.W. Yang, and J.A. Rodriguez, Surf. Sci. **296**, 164 (1993).

[19]H. Iijima, M. Kuriki, and Y. Masumoto, in Proceedings of the 8th Annual Meeting of Particle Accelerator Society of Japan, August 1-3, Tsukuba (Particle Accelerator Society of Japan, Tokyo, 2011), p. 3158.

[20]M. G. Burt and V. Heine, J. Phys. C: Solid State Phys., **11**, 961 (1978).